



Aalborg Universitet

AALBORG UNIVERSITY
DENMARK

Numerical Modeling of a Wave Energy Point Absorber

Hernandez, Lorenzo Banos; Frigaard, Peter; Kirkegaard, Poul Henning

Published in:

Proceedings of the Twenty Second Nordic Seminar on Computational Mechanics

Publication date:
2009

Document Version
Publisher's PDF, also known as Version of record

[Link to publication from Aalborg University](#)

Citation for published version (APA):

Hernandez, L. B., Frigaard, P., & Kirkegaard, P. H. (2009). Numerical Modeling of a Wave Energy Point Absorber. In L. Damkilde, L. Andersen, A. S. Kristensen, & E. Lund (Eds.), *Proceedings of the Twenty Second Nordic Seminar on Computational Mechanics* (pp. 153-156). Department of Civil Engineering, Aalborg University.

General rights

Copyright and moral rights for the publications made accessible in the public portal are retained by the authors and/or other copyright owners and it is a condition of accessing publications that users recognise and abide by the legal requirements associated with these rights.

- Users may download and print one copy of any publication from the public portal for the purpose of private study or research.
- You may not further distribute the material or use it for any profit-making activity or commercial gain
- You may freely distribute the URL identifying the publication in the public portal -

Take down policy

If you believe that this document breaches copyright please contact us at vbn@aub.aau.dk providing details, and we will remove access to the work immediately and investigate your claim.

Numerical modeling of a wave energy point absorber

Lorenzo Banos Hernandez* and Peter Frigaard

Department of Civil Engineering
Aalborg University, Aalborg, Denmark
e-mail: lbh@civil.aau.dk

Poul-Henning Kirkegaard

Department of Civil Engineering
Aalborg University, Aalborg, Denmark
e-mail: phk@civil.aau.dk

Summary The present study deals with numerical modelling of the Wave Star Energy WSE device. Hereby, linear potential theory is applied via a BEM code on the wave hydrodynamics exciting the floaters. Time and frequency domain solutions of the floater response are determined for regular and irregular seas. Furthermore, these results are used to estimate the power and the energy absorbed by a single oscillating floater. Finally, a latching control strategy is analyzed in open-loop configuration for energy maximization.

Introduction

Recent studies conclude that 0.2% of untapped ocean energy would be sufficient to cover the entire world consumption needs [9]. During the past 10 years the deployment of devices such as different buoy concepts, the OWC plants [5] and the Pelamis have given Wave Energy certain credit. For the Danish case, the Wave Star Energy device is one of the outstanding concepts [2]. This 1:10 multipoint absorber consists of 40 semispherical floaters with 20 units along each side of a squared 24m x 5m platform. Latter test rig has been grid connected near-shore with rated 5.5 kW since 2006. Hereby, the sequential floaters oscillation in heave is converted via a Power Take Off (PTO) hydraulic system into electricity. Similar to the application of pitch and stall regulation in wind energy turbines [6], the control of such a PTO is primordial. A major advantage nowadays with respect to the right control implementation is that of being able to predict down to 48h in advance the next coming waves [7].

Wave Star Energy model

In the next figure, a view of the Nissum Bredning 1:10 scale is presented in storm protection mode.



Figure 1: left: WSE view at the pier (Nissum Bredning, DK); right: WSE Floater back view

On the right figure a single floater is held fixed while water is dropping over the surface. The system is simplified through an arm around the xz plane. Hence, the floater is assumed in the following as an abstraction of a SDOF mass spring damper, with an initially free oscillating floater

mass. The excitation force F_w caused by the waves is given through $F_w = F_e + F_h + F_r$, where F_e is the excitation force, F_h the hydrostatic buoyancy force and F_r the radiation force. They are frequency dependent, and are being determined over the BEM code. Adding an explicit definition of the excitation force the governing equation of motion becomes

$$M\ddot{z} = \int_0^t h_e(t-\tau)\eta(\tau)d\tau - \left(\int_0^t k_r(t-\tau)\dot{z}(\tau)d\tau + A_{r\infty}\ddot{z} + k_h z \right). \quad (1)$$

The right hand side of (1) contains first the excitation force as a product over the Dirac impulse h_e and the surface elevation $\eta(t)$. Second and third terms constitute the radiation force due to the generated waves by the oscillation $z(t)$. It is noted that $k_r(t)$ is the radiation impulse function and $A_{r\infty}$ is the added mass value of $A(\omega)$ due to inertia, when $\omega \mapsto \infty$. The fourth term describes the Archimedes buoyancy force F_h . Latter integral terms are subject to a causal memory effect coming from the history of the waves in convoluted form over t . The calculation of the integrals is simplified over the Prony method [4]. The solution of the differential equation is the floater response $z(t)$ via a Newmark Algorithm and a Runge-Kutta Algorithm for a defined sea state over $\eta(t)$ and $F_e(t)$ to the initial conditions $z(t_0) = 0$ m and $v(t_0) = 0 \frac{m}{s}$.

Floater response

The floater response is determined with respect to the mean water level regarding the following considerations. The oceanic constraints are settled through North Sea conditions, that means short crested, $\frac{H}{L} \ll 1$, shallow waters $\frac{H}{D} \ll 1$ (water depth $\approx 2m$). The Cummins decomposition of wave forces [3] is used for a unidirectional JONSWAP wave spectra (through the yz plane), whereas zero friction viscous losses apply.

Furthermore, the input values for the Boundary Element code are a geometry with a semisphere (symmetry to x,y), the diameter of $1m$ and a draught D of 0.5 m. Herewith, a quad mesh with 256 panels and 297 points is generated over the wetted surface. For the numerical model the following parameters are used

- Floater mass: $M = 235$ kg
- Significant Wave Height $H_s : 1.2m$
- Wave Period T ranging from $0.1 : 0.27 : 21$ s

For the later control implementation, a mechanical Stiffness for the floater arm is defined over $K_c = 10000 \frac{kg}{s^2}$. Thereby, the mechanical damping C_c is first exerted as a constant ($C_c = 10000 \frac{kg}{s}$) and then as a non-linear damping ($C_c \text{sign}(\dot{z})|\dot{z}|$).

Power absorption

The power absorbed by the oscillating floater is calculated for a resonant situation. The next equation reflects the solution of Eq.(1) for a complex floater response, where the mechanical resistance is damped out by the water ($C_c = C_h$):

$$H(j\omega) = \frac{\hat{F}_e(\omega)\hat{\eta}(\omega)}{-(m + m_h(\omega))\omega^2 + j\omega(C_c + C_h(\omega)) + k_h(\omega) + k_c} \quad (2)$$

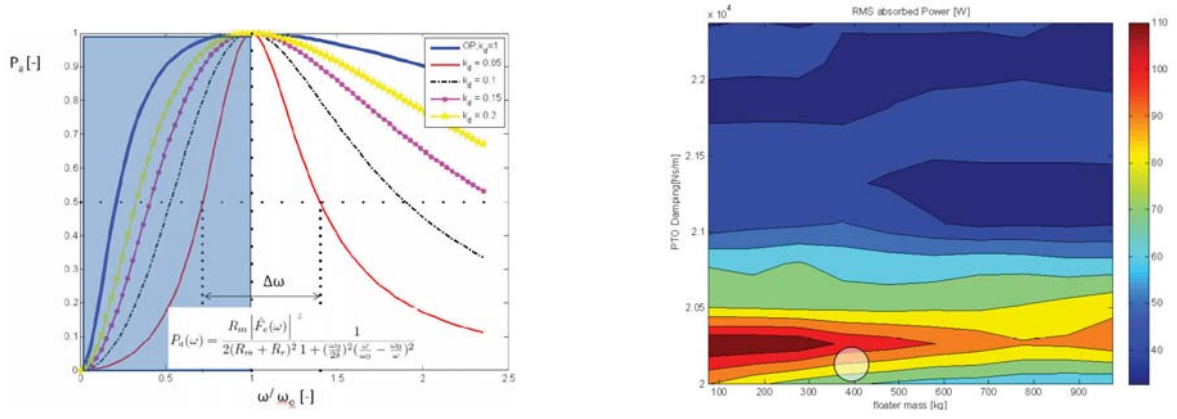


Figure 2: non-dimensional Absorbed Power for Figure 3: Absorbed RMS [W] over floater mass M and mechanical damping C_c

Fig.(2) shows the non-dimensional behavior of absorbed power P_a over the frequency range $\frac{\omega}{\omega_0}$. Therefore, the damping ratio k_d is varied linearly in 0.05 steps up to the operating range (blue curve), corresponding to the regular sea state of latter simulations. The higher the damping ratio, the faster the power increases up to resonance frequency, where $\frac{\omega}{\omega_0} = 1$. For higher frequencies, this linearization also results in a wider bandwidth ($\Delta\omega$). In order to quantify the Power absorbed, the Root mean square RMS is calculated as a function of mass and PTO damping. The contour plots are shown in Fig. (3)

Maximal Power between 110 W and 165 W is obtained for a mass variation of 70 - 500 kg (x-axis). The PTO damping on the y-abscissa variates from 2 - $2.05 \frac{kg}{s}$ for exciting loads ranging from -72.47 N to 226.98 N.

Finally, a latching control system strategy is applied for the linear damping case in regular waves, that locks and releases the body motion within given intervals. The objective is to tune the velocity to be in phase with the excitation force, while keeping the resonance condition. Results to this discrete phase control are presented in the next graphs.

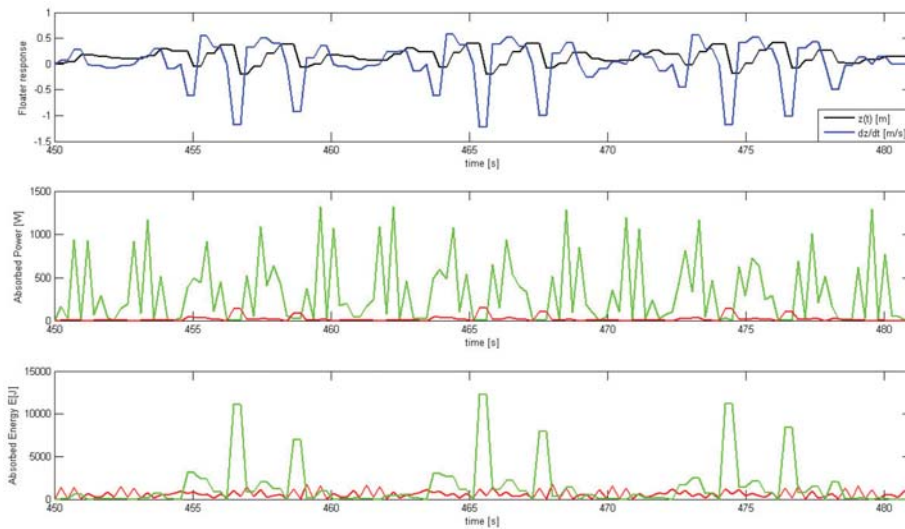


Figure 4: Floater response [m], Instantaneous absorbed Power [W] and available Energy [J]

The simulation results are fixed to a 31s interval after the transient of the floater response vanishes (nearly 450 s, with $\delta t = 0.24s$). As it can be seen in Fig. (4) the position is held constant during almost 1s latching intervals. The Power absorbed in the second plot compares the uncontrolled case

(red curve) with the latched strategy (green curve). Same procedure applies on the third subplot, where the wave energy absorption in J is compared for both cases. It is noted that the position, the absorbed power and wave energy correlate closely for time intervals with peak performance (e.g. at $t = 457, 459$ or $466s$).

Conclusion

The study introduces a standardized approach within the field of control algorithms for point absorbers. In time domain, the single body model performs with increased computational efficiency in comparison to previous analysis done in FORTRAN. The hydrodynamics coefficients acquisition is similar to commercial software examples, like WAMIT [1]. The floater response reveals the characteristic behavior of a second order delay system in control theory. Moreover, the power absorption ratio on Fig.(2) shows the significance of fitting the operative range of the device to a narrow bandwidth close to resonance frequency. The parametrization of mass and damping indicate that an increase of the mass might avoid possible floater slamming for maximum power. For instance a mass of nearly 400 kg and a damping value of nearly $2e4 \frac{kg}{s}$ can still achieve 80-100 W(RMS) per floater (white circle on Fig. (3)). Through the applied control strategy, it can be seen that the power can be amplified significantly (in the order magnitude of 2-3 times the latched RMS power). Though, the peaks of nearly 1 kW per floater are quite unrealistic in comparison to the range calculated over Fig. (3). Despite of the stability analysis done, further improvements may be achieved through other control strategies that might be applied in order to smoothen the power output. Furthermore, the extension to the multibody formulation and the inclusion of stochastic disturbances is of interest for the WSE development [8].

References

- [1] Falnes, J. Ocean Waves and Oscillating Systems. *Cambridge*, ISBN 982-207-002-0, (2002).
- [2] Kramer, M. Internal Reports on Hydrodynamics and Structural design. Wave Star Energy, (2004-2009).
- [3] Cummins, W.E. The impulse response function in ship motions. *Schiffstechnik*, 491-502, (1962).
- [4] de Backer, G. Basics in numerical time domain simulation of a heaving point absorber. *Ghent University, Trainee report*, , (2007).
- [5] Heath, T.V. The Development of a Turbo-Generation System for Application in OWC Breakwaters. *Proceedings of the 7th European Wave and Tidal Energy Conference*, Wavegen, (2007).
- [6] Chen, Z., Blaabjerg, F., Ackermann, T. et al. Offshore Wind Power. *Twidell*, ISBN 982-207-002-0, (2009).
- [7] Rhinefranka, K. Agamloha, E.B. et al. Novel ocean energy permanent magnet linear generator buoy. *OSU, School of Electrical Engineering*, p.1-5, (2005).
- [8] Wave Star Energy A/S <http://www.wavestarenergy.com>.
- [9] Brekken, T. The promise of wave power. IET Presentation, AAU. *Oregon State University*, p.1-3, (2009).